

603949

AD

WVT-11-6404

MAY 1964

THE EFFECT OF FERRITE ON THE MECHANICAL PROPERTIES
OF A PRECIPITATION HARDENING STAINLESS STEEL

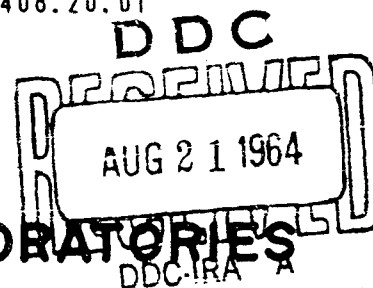
TECHNICAL REPORT

BY

V. J. COLANGELO
METALLURGIST

47p
hc-2.00
mf-0.50

AMCMS CODE NO. 4230.15.7408.20.01



WVT-11-6404

BENÉT R & E LABORATORIES
WATERVLIET ARSENAL
WATERVLIET - NEW YORK

DISTRIBUTED BY
OFFICE OF TECHNICAL SERVICES
DEPARTMENT OF COMMERCE
1200 S. EADS ST.
ARLINGTON, VA.
ATTN: OTS STOCK

DISPOSITION

This report will be destroyed by the holder when no longer required.

ADDITIONAL COPIES

Qualified requesters may obtain copies of this report from the Defense Documentation Center Headquarters.

Copies available at Office of Technical Services \$1.25

The findings in this report are not to be construed as an official Department of the Army position.

THE EFFECT OF FERRITE ON THE
MECHANICAL PROPERTIES OF A PRECIPITATION
HARDENING STAINLESS STEEL

Abstract

The primary object of this study was to determine the effect of ferrite and its orientation upon the mechanical properties of a precipitation hardening stainless steel with particular attention to the short transverse properties. The investigation consisted of four major parts: the preliminary investigation of billet properties; the effect of forging reduction and ferrite content upon mechanical properties; the effect of notch orientation upon impact strength and the relationship of heat composition to ferrite content.

Low ductility and impact strength in the short transverse direction were found to be associated with the orientation and shape of the ferrite plates.

It was also determined that notch orientation had a direct effect upon the values obtained in impact testing.

The overall investigation showed that high ferrite contents in general had a deleterious effect upon mechanical properties and that the ferrite content could be minimized by exercising rigorous control of the heat composition.

Cross-Reference
Data

Precipitation Hardening
Stainless Steel
Mechanical Properties

Ferrite, Effect of

Anisotropy

TABLE OF CONTENTS

	Page
Abstract	1
Conclusions	5
Recommendations for Further Study	6
List of Symbols	7
Introduction	8
Objective	9
Method of Procedure	9
A. Preliminary Investigation of Billet and Forging Properties	9
B. Effect of Forging Reduction and Ferrite Content Upon Mechanical Properties	10
C. Effect of Notch Orientation Upon Impact Strength	11
D. Relationship of Ferrite Content to Heat Composition	14
Results	14
Discussion of Results	14
References	35
Appendix	42
Distribution List	45

FIGURES

1. Schematic Representation of Forging Procedure	10
2. Location of Test Specimens Relative to Forging	12
3. Schematic Representation Illustrating Charpy V-Notch Orientation in Longitudinal, Transverse and Short Transverse Directions	12
4. Diagram Illustrating Relative Locations of Micro Specimens	13
5. Schematic Representation Illustrating Orientation in 3" x 1" Forging	13

FIGURES (Cont'd.)

	Page
6. Ductility as a Function of Forging Reduction Heat D	16
7. Ductility as a Function of Forging Reduction Heat E	17
8. Longitudinal Tensile from 5" Thick Forging of Heat D	18
9. Transverse Tensile from 5" Thick Forging of Heat D	18
10. Short Transverse Tensile from 5" Thick Forging of Heat D	18
11. Longitudinal Tensile from 3" Thick Forging of Heat D	19
12. Transverse Tensile from 3" Thick Forging of Heat D	19
13. Short Transverse Tensile from 3" Thick Forging of Heat D	19
14. Longitudinal Tensile from 1 1/2" Thick Forging of Heat D	20
15. Transverse Tensile from 1 1/2" Thick Forging of Heat D	20
16. Short Transverse Tensile from 1 1/2" Thick Forging of Heat D	20
17. Shape and Orientation of Ferrite Plates Heat D - 5" Thick Forging	21
18. Shape and Orientation of Ferrite Plates Heat D - 3" Thick Forging	22
19. Shape and Orientation of Ferrite Plates Heat D - 1 1/2" Thick Forging	23
20. Shape and Orientation of Ferrite Plates Heat E - 5" Thick Forging	24
21. Shape and Orientation of Ferrite Plates Heat E - 3" Thick Forging	25

FIGURES (Cont'd.)

	Page
22. Shape and Orientation of Ferrite Plates Heat E - 1 1/2" Thick Forging	26
23. Ferrite Content as a Function of Chromium Equivalent	27
24. Short Transverse Tensile Heat E - 5" Thick Forging	30
25. Short Transverse Tensile Heat E - 3" Thick Forging	30
26. Short Transverse Tensile Heat D - 3" Thick Forging	31
27. Short Transverse Tensile Heat D - 1 1/2 Thick Forging	31
28. Fracture Surface of Longitudinal and Transverse Charpy V-Notch Specimens	33
29. Photomicrograph Illustrating the Grid Method	44

TABLES

I. Mechanical Properties of Billet Stock	36
II. Mechanical Properties of 1 1/2" Thick Flat Forgings	36
III. Mechanical Properties of 5" Thick Forging from Heat D	37
IV. Mechanical Properties of 3" Thick Forging from Heat D	37
V. Mechanical Properties of 1 1/2" Thick Forging from Heat D	38
VI. Mechanical Properties of 5" Thick Forging from Heat E	38
VII. Mechanical Properties of 3" Thick Forging from Heat E	39
VIII. Mechanical Properties of 1 1/2" Thick Forgings from Heat E	39
IX. Effect of Notch Orientation Upon Impact Strength	40

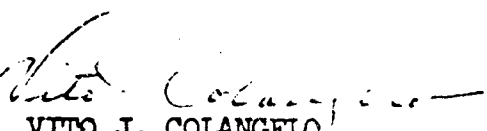
CONCLUSIONS

1. Ferrite exerts a marked effect on the ductility obtainable from a flat forging. The shape and orientation of the ferrite produces an anisotropic condition with respect to the ductility in the three directions. The percentage of elongation and reduction in area is greatest in the longitudinal direction while the lowest results were obtained in the short transverse direction.


2. As the amount of forging reduction increases, a point is reached at which there is a sharp decrease in the short transverse ductility. With higher ferrite contents, this point is reached with less reduction. This point of divergence is coincident with the achievement of a planar distribution of ferrite.

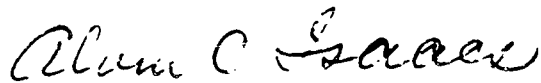
3. Notch orientation exerts a definite effect upon impact strength. Higher results are obtained when the notch axis of the impact specimen is parallel to the plane of the ferrite plates. The opposite result is encountered when the notch axis is perpendicular. This effect occurs regardless of test direction but is less pronounced in the transverse direction.

4. There is essentially a linear relationship between ferrite content and chromium equivalent. Heats having a high chromium equivalent tend toward higher ferrite contents. When the chromium equivalent becomes negative (positive nickel equivalent) there is a tendency toward retained austenite, the presence of which is detrimental.


VITO J. COLANGELO
Metallurgist

Approved:


R. E. Weigle
Chief Scientist


ALVIN C. ISAACS
Lt Col, Ord Corps
Chief, Benet R&E Laboratories

RECOMMENDATIONS FOR FURTHER STUDY

In the course of this investigation it became evident that further study was indicated in certain areas.

The distinct anisotropy in ductility shown in the three test directions indicates that the investigation of other properties such as fatigue strength would be warranted.

It is believed that since this anisotropy is the direct result of the orientation of the ferrite present, that the conclusions drawn might be applied to other alloys having similar microstructures. It is also believed that alloys having secondary phases, other than ferrite, are capable of exhibiting a similar anisotropy if these phases are present in sufficient quantities and if the forging practice is such to promote directional orientation of the second phase. The validity of these beliefs, however, should be supported by the results of an appropriate investigation.

LIST OF SYMBOLS

C	Carbon
Mn	Manganese
Si	Silicon
Cr	Chromium
Ni	Nickel
Mo	Molybdenum
N	Nitrogen
M_s	Start of martensite transformation
M_f	Completion of martensite transformation
A.C.	Air cool
A.W	Air warm
W.Q.	Water quench

INTRODUCTION

The precipitation hardening stainless steels were developed to fulfill a need for high strength corrosion resistant alloys. In the annealed condition they are soft and ductile and possess many of the desirable characteristics of the austenitic stainless steels. In the hardened condition, the alloys exhibit the high strength and hardness of the martensitic stainless steels.

The alloy under consideration in this investigation has a nominal composition as follows:

C	Mn	Si	Cr	Ni	Mo	N
0.13	0.95	0.25	15.50	4.30	2.75	0.10

The hardening mechanism is identical to that of other hardenable steels in that it depends upon the transformation of austenite to martensite.

This alloy, because of its annealed structure and its ability to be hardened, combines the desirable forming and corrosion properties of the austenitic grades with the high hardness and strength levels attainable with the hardenable grades.

The reason for this apparent duplicity of properties can be explained by considering a basic metallurgical difference between the hardenable stainless steels and those of the austenitic group. Both types are austenitic at 1800° F, but while the martensitic grades transform to martensite upon rapid cooling to room temperature, the austenitic grades remain austenitic even when cooled to temperatures below room temperature. The major difference then is in the degree of austenite stability. This stability can quantitatively be described by the Ms temperature. The Ms being defined as that temperature at which austenite begins to transform to martensite. The austenitic grades for example may be cooled to -300° F without producing significant quantities of martensite. The hardenable stainless steels on the other hand have an Ms temperature in the vicinity of 400 to 700° F. In cooling to room temperature, these alloys traverse the entire Ms - Mf range and show almost complete transformation to martensite. The semi-austenite stainless steel, however, occupies an intermediate position with respect to its austenite stability. The analysis is so balanced that the Ms temperature lies at or slightly above room temperature. The resulting alloy retains much of its austenite at room temperature and yet responds to hardening heat treatments.

Achieving this delicate balance of elements is therefore of great importance. Slight imbalances of the equivalent Cr - Ni ratios frequently result in the presence of delta ferrite. It is the effects of this ferrite with which we are concerned, more specifically the effect of the quantity and ferrite orientation upon mechanical properties, particularly ductility.

OBJECTIVE

The objective of this project was to determine the effect of ferrite and its orientation upon the mechanical properties of a precipitation hardening stainless steel.

METHOD OF PROCEDURE

A. Preliminary Investigation of Billet and Forging Properties

In order to determine the effect of ferrite on billet properties, billet stock from three heats with various ferrite contents were utilized. From this material, tensile specimens were obtained in the transverse and longitudinal directions and given the following heat treatment.

1375° F (3 hrs.) A.C.
+
1710° F (1 hr.) W.Q.
+
-100° F (3 hrs.) A.W.
+
850° F (3 hrs.) A.C.

Forgings were made from these same heats, the purpose being to determine what effect, if any, the ferrite might have upon the mechanical properties. These forgings were made in such a manner as to elongate the ferrite in the longitudinal and transverse directions.

The method of forging was as follows: A 6 inch long section was cut from a 6 inch square billet of Heat A. This was then flat forged to 1 1/2 inch thick. Work was done from one direction only with no edging passes as shown in Figure 1. Forging was begun from a furnace temperature of 2150° F. Heats B and C (12 inch square billets) were treated in a similar manner except that quartered sections (approximately 6 inch square by 6 inch long) were used in place of full cross sections. Tensile specimens were taken from the resultant flattened forgings in the transverse and short transverse directions and heat treated as previously described.

Microscopic examination of the fractures was made in all cases.

B. Effect of Forging Reduction and Ferrite Content Upon Mechanical Properties

It was decided to evaluate the effect of forging reduction upon heats of various ferrite content. Heat D was selected because of its

* Throughout this work the short transverse direction will be taken to mean the shortest dimension in a transverse section and the transverse direction to be the greatest dimension in a transverse section.

1. CUT PIECE FROM
BILLET.

2. FORGE NORMAL
TO LONGITUDINAL
AXIS.

3. FINISH FORGING.

Figure 1. Schematic Representation of Forging Procedure

relatively low ferrite content (3%) and Heat E because the ferrite content was considerably higher (15%). The procedure in both cases was as follows: Four 6 inch long sections were cut from an 8 inch square billet. The first section was used for longitudinal and transverse tests representative of the original billet size. The remaining sections were then flat forged as previously described to 5, 3, and 1 1/2 inches thick respectively. From each forging tensile and impact tests were taken in the longitudinal (L), transverse (T), and short transverse (S) directions from center, mid-radius and edge locations as illustrated in Figure 2.

1425° F (2 hrs.) W.Q.

+

1750° F (1 hr.) W.Q.

+

-100° F (3 hrs.) A.W.

+

1000° F (3 hrs.) A.C.

This deviation from the heat treatment previously described was made for the following reason. The former heat treatment favors high strength at some sacrifice in ductility. Since the preliminary data indicated that ductility was adversely affected by the ferrite it was decided to use a heat treatment which did not further restrict this property.

The fractures were examined microscopically and representative microphotographs taken.

The type of impact specimens used were Charpy V-notch specimens. In each case the notch axis was parallel to the plane of the long transverse direction as shown in Figure 3, since it was anticipated that a variation in notch orientation might produce a change in test results, thus, introducing another variable factor.

Three micro-specimens were cut from each forging representing the top view (longitudinal), side view (longitudinal), and front view (transverse) of the forging. The location of the micro-specimens relative to the forging is shown in Figure 4. These specimens were etched, photographed, and mounted to illustrate the size, shape and distribution of the ferrite plates in three dimensions.

C. Effect of Notch Orientation Upon Impact Strength

To test the premise that notch orientation effects impact strength, (3 inch x 1 inch) flats were forged from two heats. Transverse and longitudinal impact tests were then obtained with the notch axes parallel to the long transverse plane. Similar tests were also conducted with the notch axes perpendicular to the long transverse plane. The orientation of the specimens relative to the forging is shown in Figure 5.

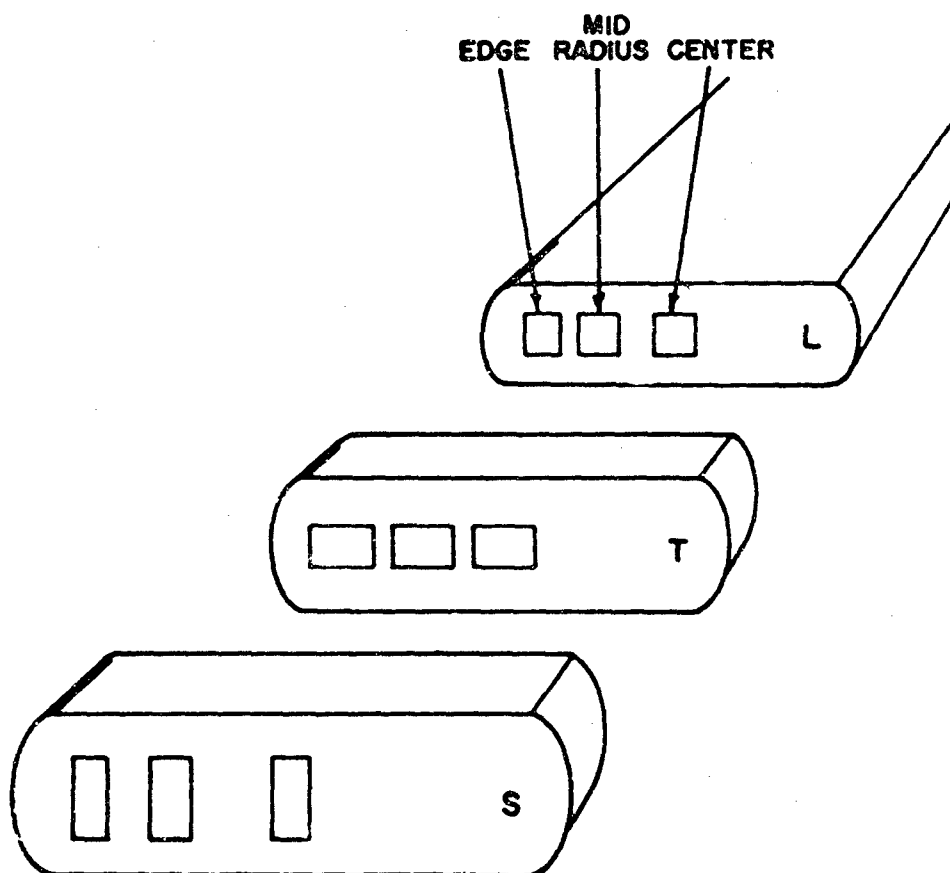


Figure 2. Location of Test Specimens Relative to Forging

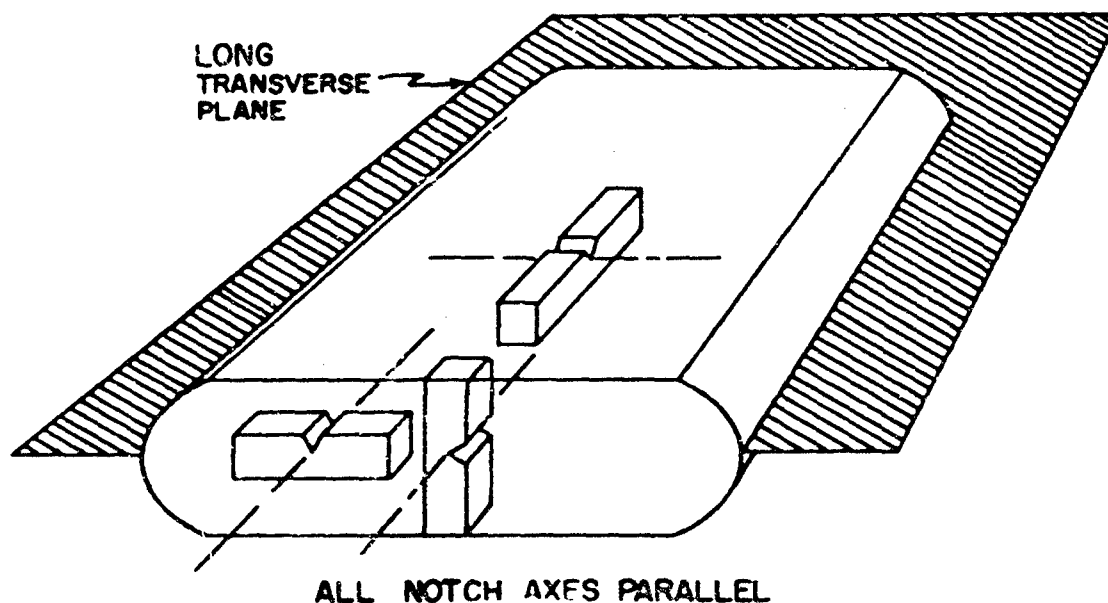


Figure 3. Schematic Representation Illustrating Charpy V-Notch Orientation in Longitudinal, Transverse and Short Transverse Directions

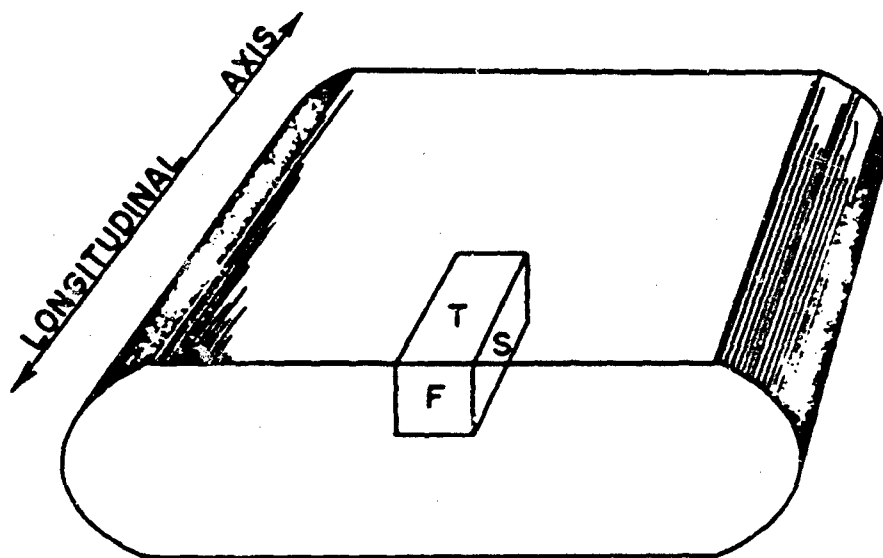


Figure 4. Diagram Illustrating Relative Locations of Micro Specimens

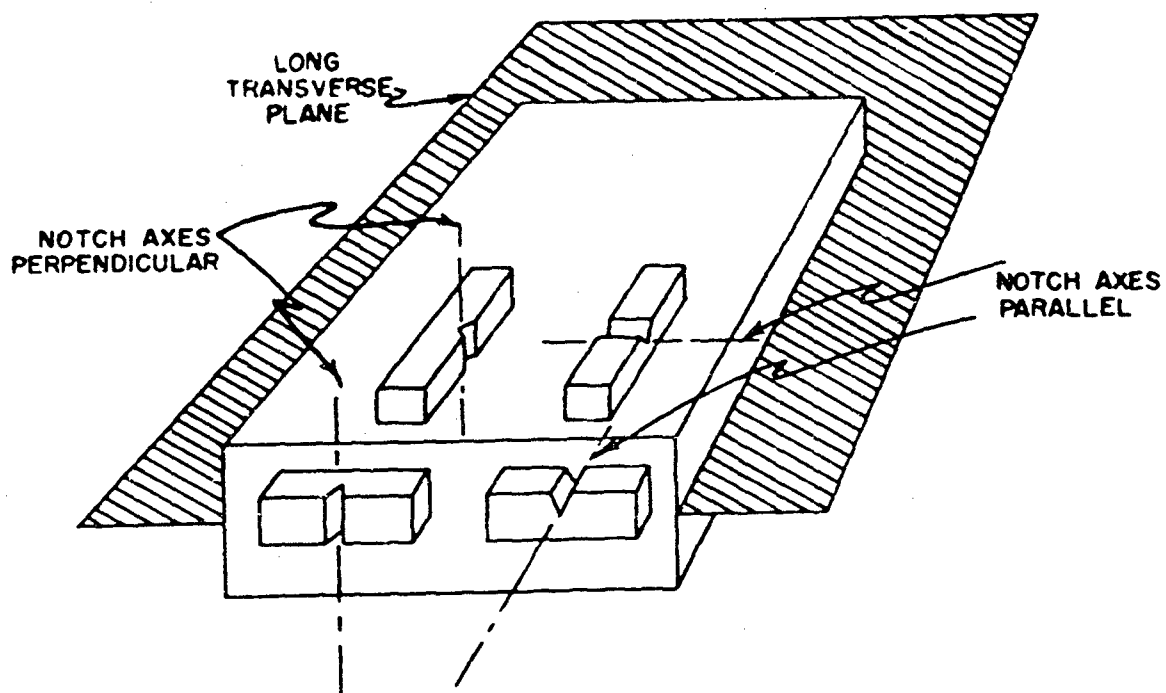


Figure 5. Schematic Representation Illustrating Orientation in 3"x1" Forging

D. Relationship of Ferrite Content to Heat Composition

Samples from eighteen randomly selected heats were chemically analyzed and the percentage of ferrite present was determined using a point count grid method. This method is presented in detail in the Appendix.

The Chromium - Nickel balance for each heat was calculated using a modified Theilman equation. The values employed per percent of element are as follows:

C (-40)	Si (+6)
Ni (-4)	Cr (+1)
Mn (-2)	Mo (+4)
N (-30)	

The Chromium Equivalent for each heat was then plotted against the corresponding ferrite content.

RESULTS

The results of the tests performed and previously described are presented herein. In addition to the test results the following general information is also presented because it is believed that such information is pertinent to the interpretation of the results.

All tensile specimens were sub-standard size of 0.250 inch diameter except where otherwise indicated.

The impact specimens used were Charpy V-notch specimens, prepared and tested according to ASTM specifications and designations.

A. Preliminary Investigation of Billet and Forging Properties

The results of the tensile tests conducted on billet material in the preliminary investigation are presented in Table I.

Table II shows the mechanical properties in the transverse and short transverse directions obtained when sections from these billets were flat forged to 1 1/2 inches thick. The tensile specimens in the short transverse direction were 0.125 inch diameter with a reduced section 0.5 inch in length.

B. Effect of Forging Reduction and Ferrite Content Upon Mechanical Properties

Tables III, IV, V show the tensile and impact test results from heat D (low ferrite). The corresponding results from heat E (high ferrite) are given in Tables VI, VII, VIII. Figures 6 and 7 graphically illustrate the effect of forging reduction upon the ductility of the low and high ferrite heat respectively.

As was previously mentioned, the fractures were examined metallographically and Figures 8 through 16 are presented to show the appearance of the fracture from the variously oriented tensiles from each forging of heat D. Micros from heat E are omitted since they are identical except for having greater concentration of ferrite.

Figures 17 through 22 are three-dimensional representations illustrating the size, shape and orientation of the ferrite particles from each forging of both heats.

C. Effect of Notch Orientation Upon Impact Strength

The impact data obtained by varying the notch orientation is presented in Table IX. Macro and micro photographs were taken but are more suitably presented in the Discussion.

D. Relationship of Ferrite Content to Heat Composition.

The chemical analysis, ferrite content and chromium equivalent for each heat is tabulated in Table X. This data is shown in Figure 23 which is a plot of ferrite content versus the resultant chromium equivalent.

DISCUSSION OF RESULTS

A. Preliminary Investigation

The preliminary investigation of billet properties is rather inconclusive. Examination of the data presented in Table I revealed that the ductility of Heat A was good while that of the other two heats is lower. The two possible explanations are: the larger billet size of the latter heats did not allow sufficient grain refinement or the presence of greater amounts of delta ferrite in these heats exerts a markedly deleterious effect. In this case the amount of ferrite is believed to be relatively unimportant since Heat A containing 5% ferrite exhibited good properties while Heat B containing only a slightly greater amount showed low ductility. The poor properties are undoubtedly due to lack of sufficient grain refinement.

The data from the 1 1/2 inch thick forgings of this material showed that the ductility in the short transverse direction is quite poor

HEAT D

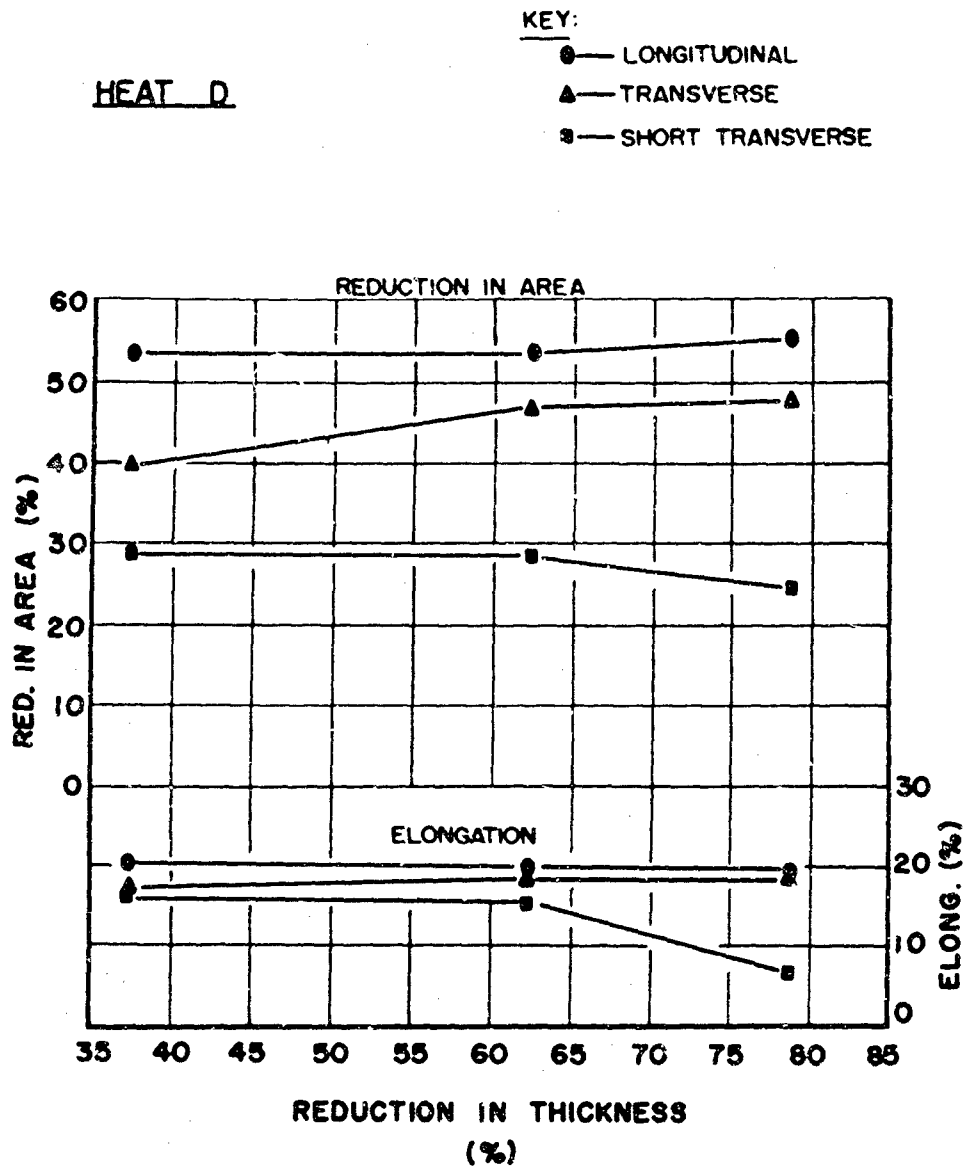


Figure 6. Ductility vs Reduction in Thickness

HEAT E

KEY:

- — LONGITUDINAL
- ▲ — TRANSVERSE
- — SHORT TRANSVERSE

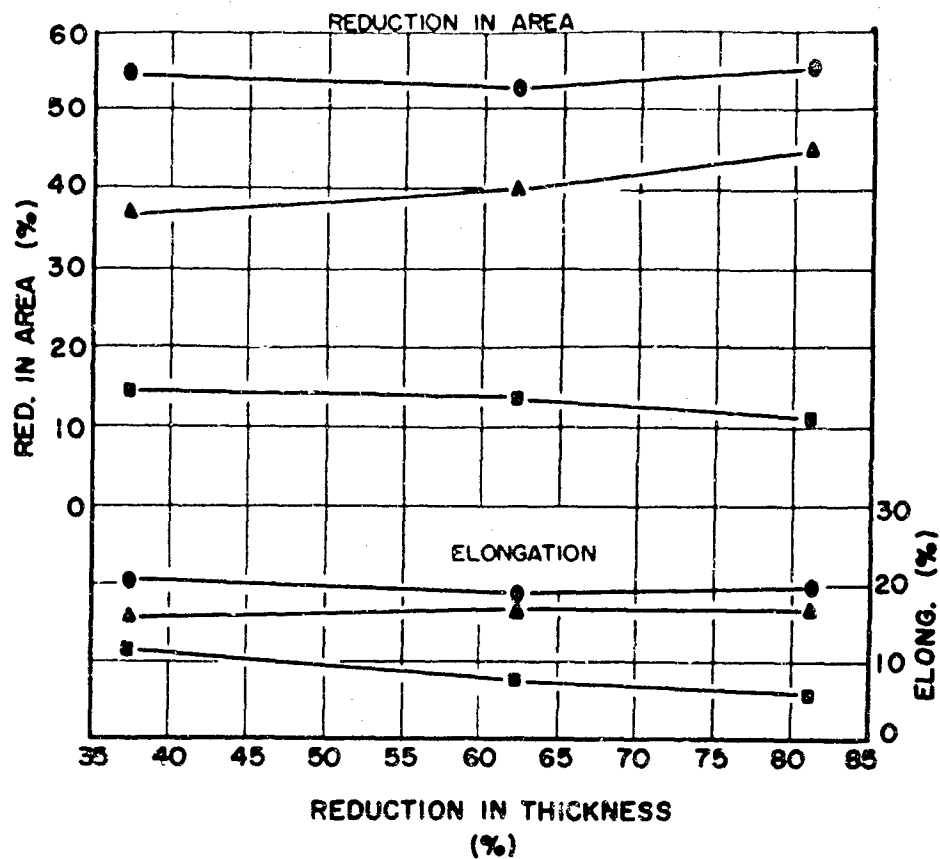


Figure 7. Ductility vs Reduction in Thickness

Heat D ---- 5" Thick Forging
Longitudinal Section Through Fracture

Figure 8
Longitudinal tensile
Etchant: HCl-Picral
100X

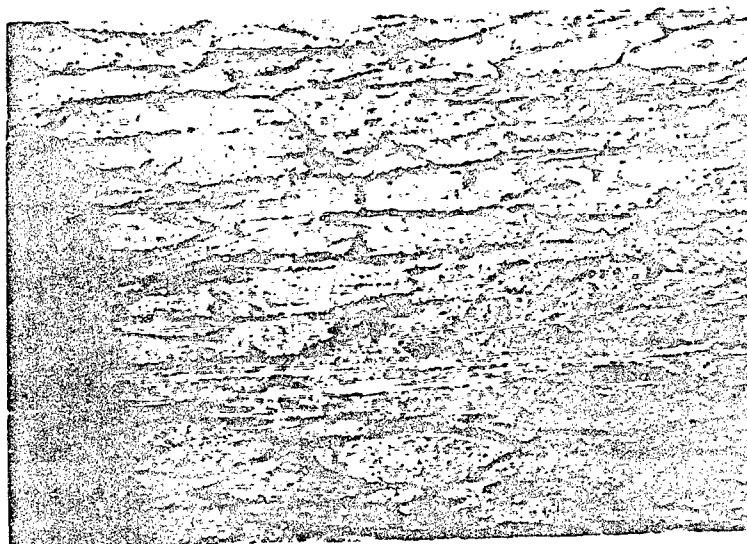
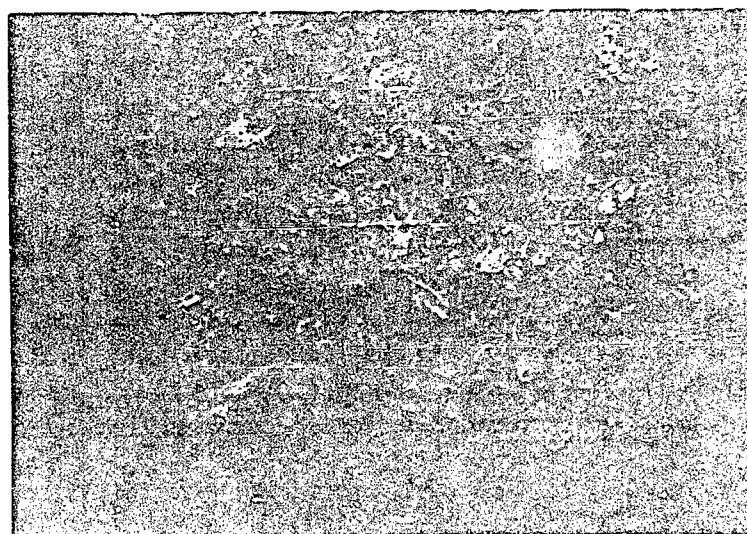


Figure 9
Transverse tensile
Etchant: HCl-Picral
100X



Figure 10
Short Transverse
tensile
Etchant: HCl-Picral
100X



Heat D ---- 3" Thick Forging
Longitudinal Section Through Fracture

Figure 11
Longitudinal tensile
Etchant: HCl-Picral
100X

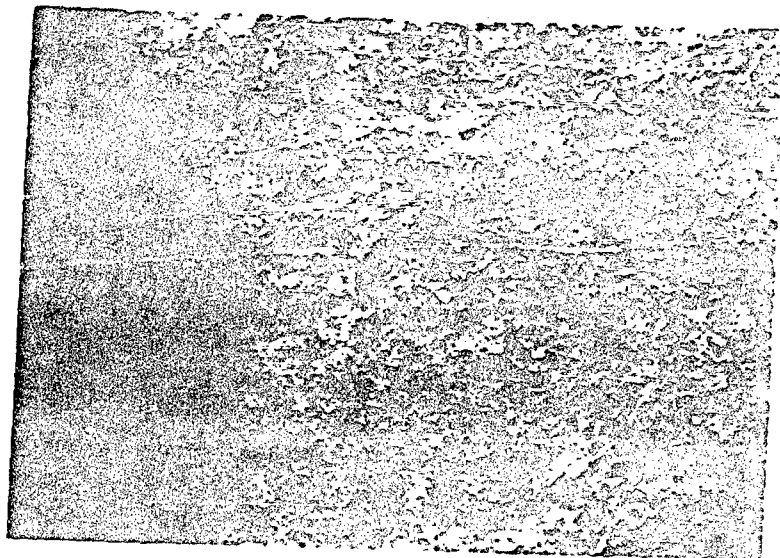


Figure 12
Transverse tensile
Etchant: HCl-Picral
100X

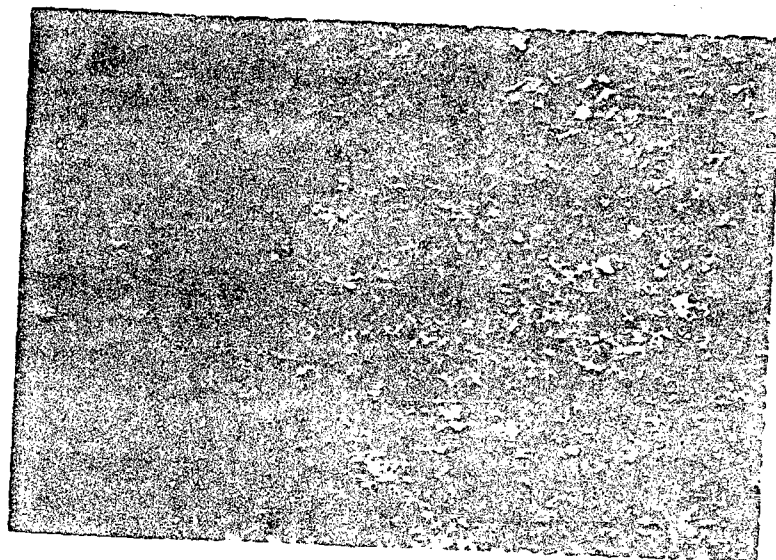
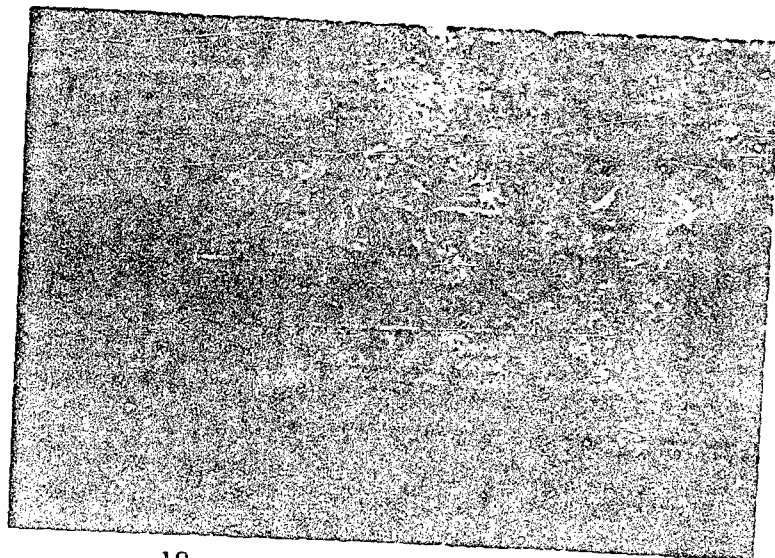


Figure 13
Short Transverse
tensile
Etchant: HCl-Picral
100X



Heat D ---- 1 $\frac{1}{2}$ " Thick Forging
Longitudinal Section Through Fracture

Figure 14
Longitudinal tensile
Etchant: HCl-Picral
100X

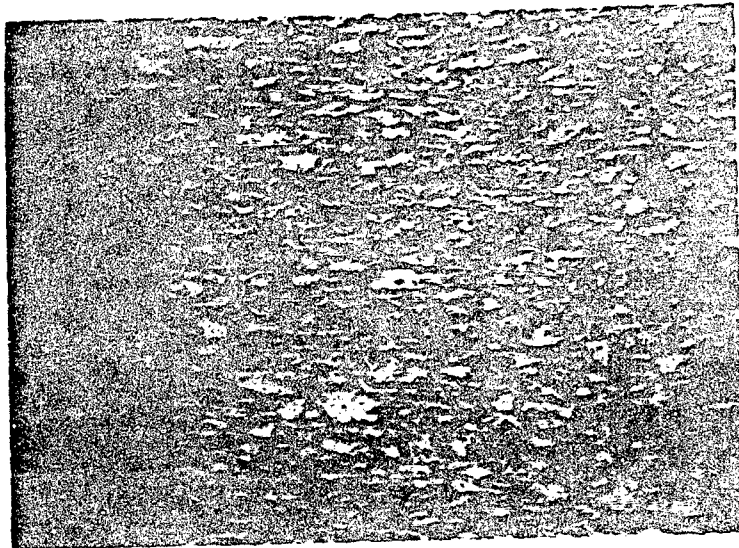


Figure 15
Transverse tensile
Etchant: HCl-Picral
100X

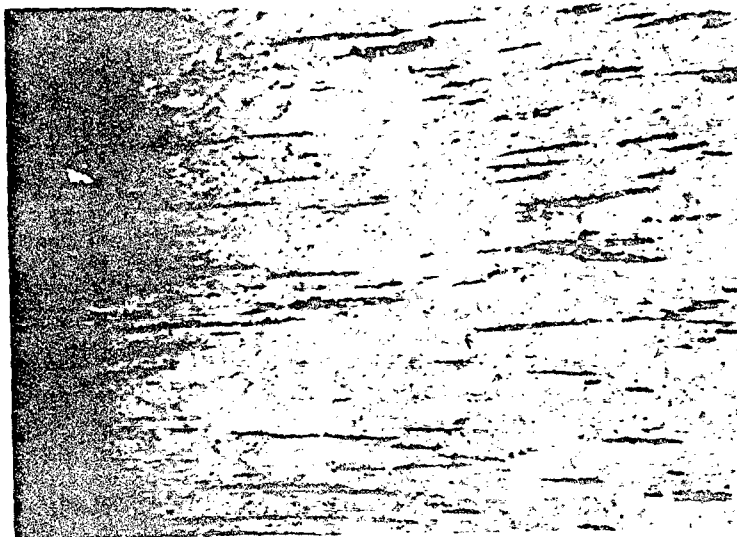
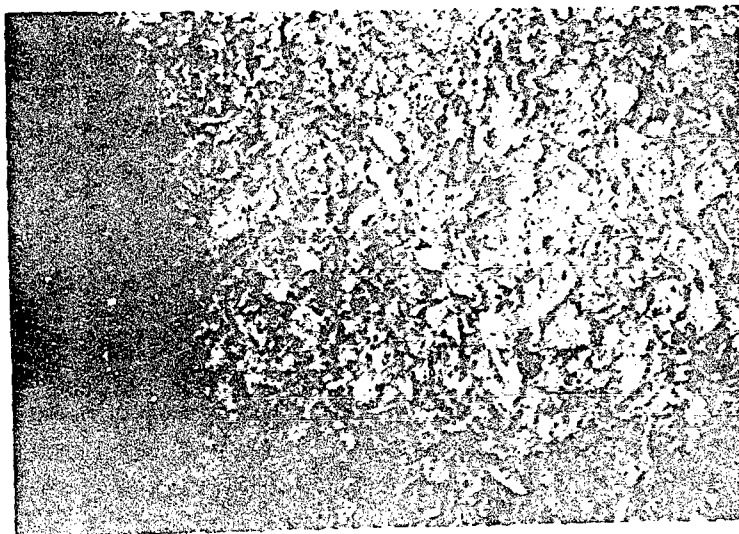
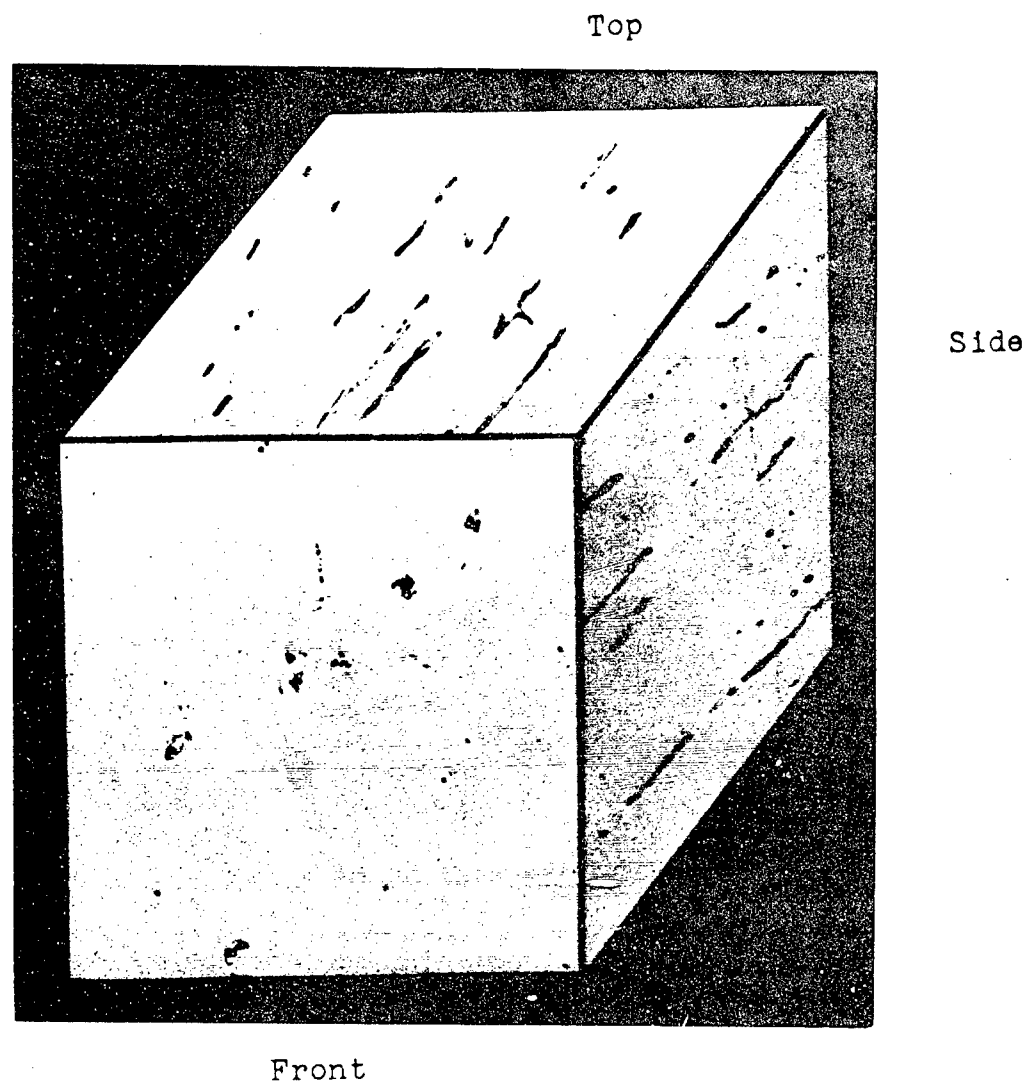


Figure 16
Short Transverse
tensile
Etchant: HCl-Picral
100X



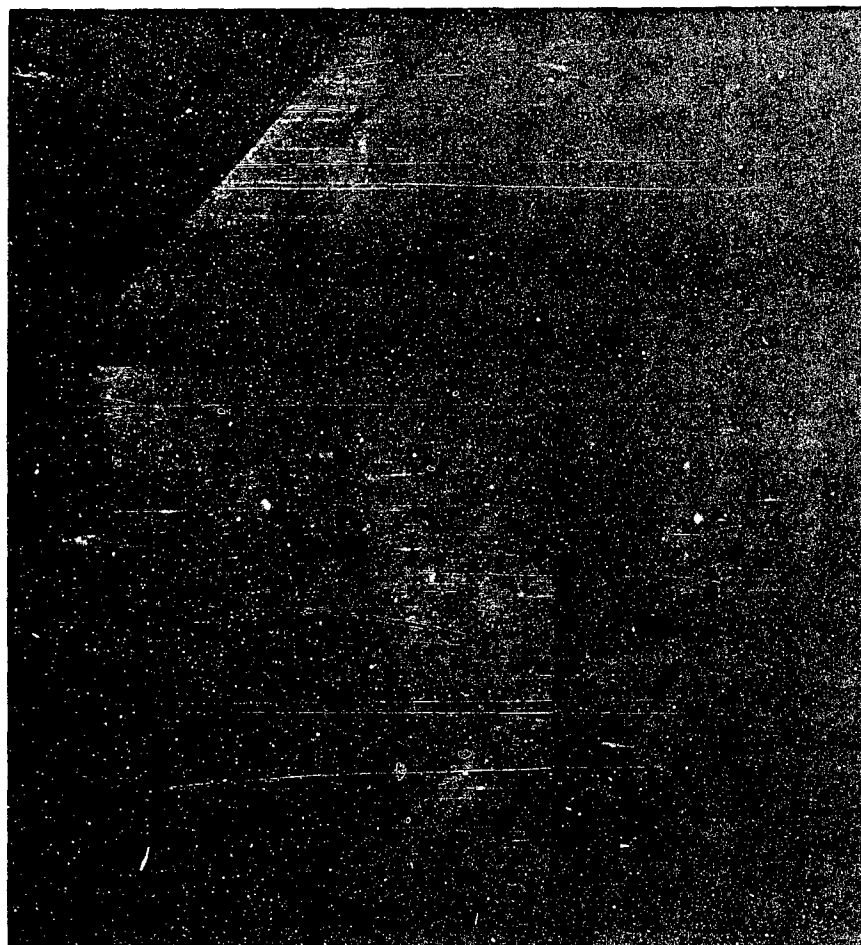


Heat D ---- 5" Thick Forging

100X

Figure 17. Composite Photograph Illustrating Shape and Orientation of Ferrite Plates

Top



Side

Front

Heat D ---- 3" Thick Forging

100X

Figure 18. Composite Photograph Illustrating Shape and Orientation of Ferrite Plates

Top



Side

Front

Heat D ---- $1\frac{1}{2}$ " Thick Forging

100X

Figure 19. Composite Photograph Illustrating Shape and Orientation of Ferrite Plates

Top



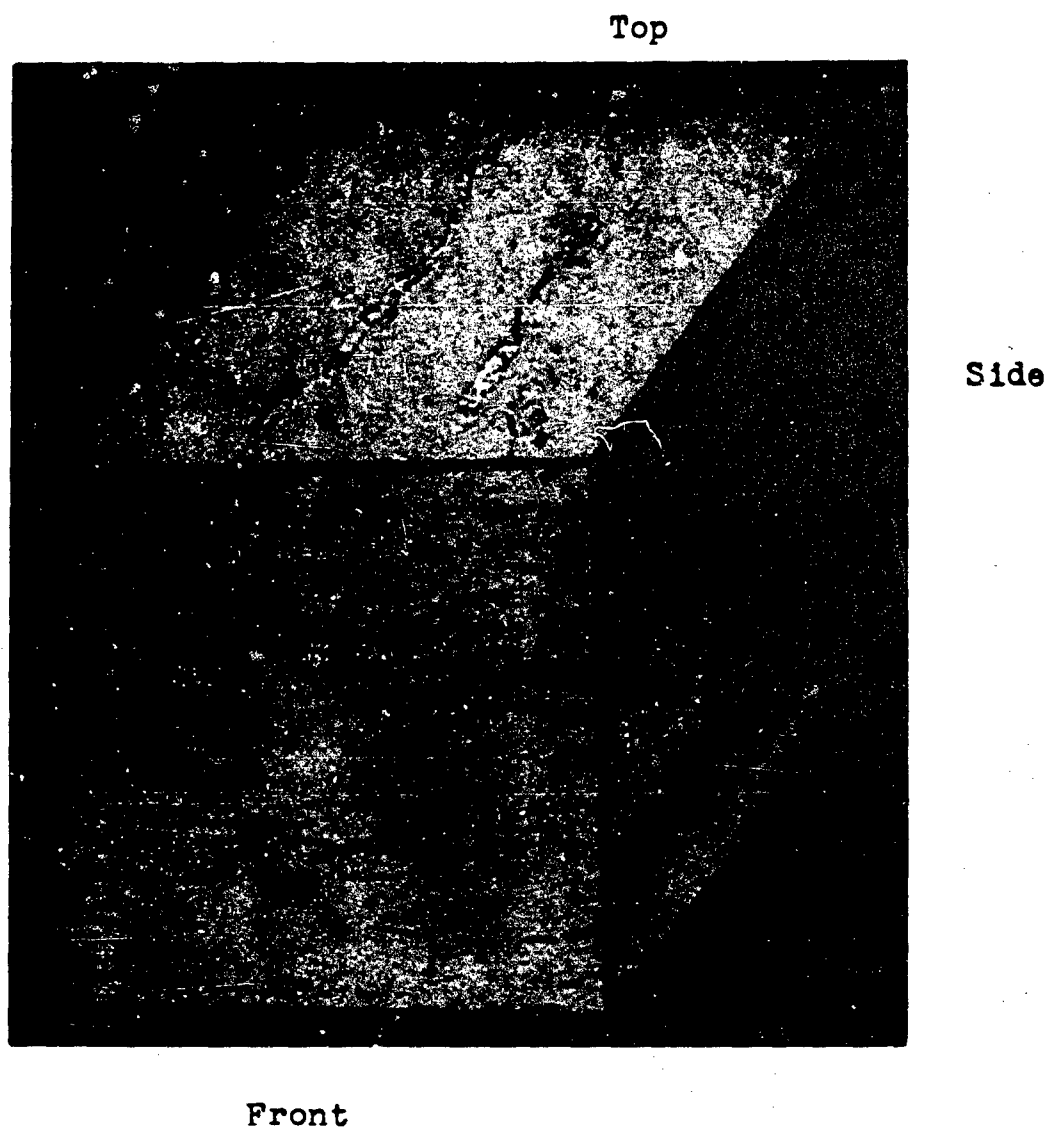
Side

Front

Heat E ---- 5" Thick Forging

100X

Figure 20. Composite Photograph Illustrating Shape and Orientation of Ferrite Plates

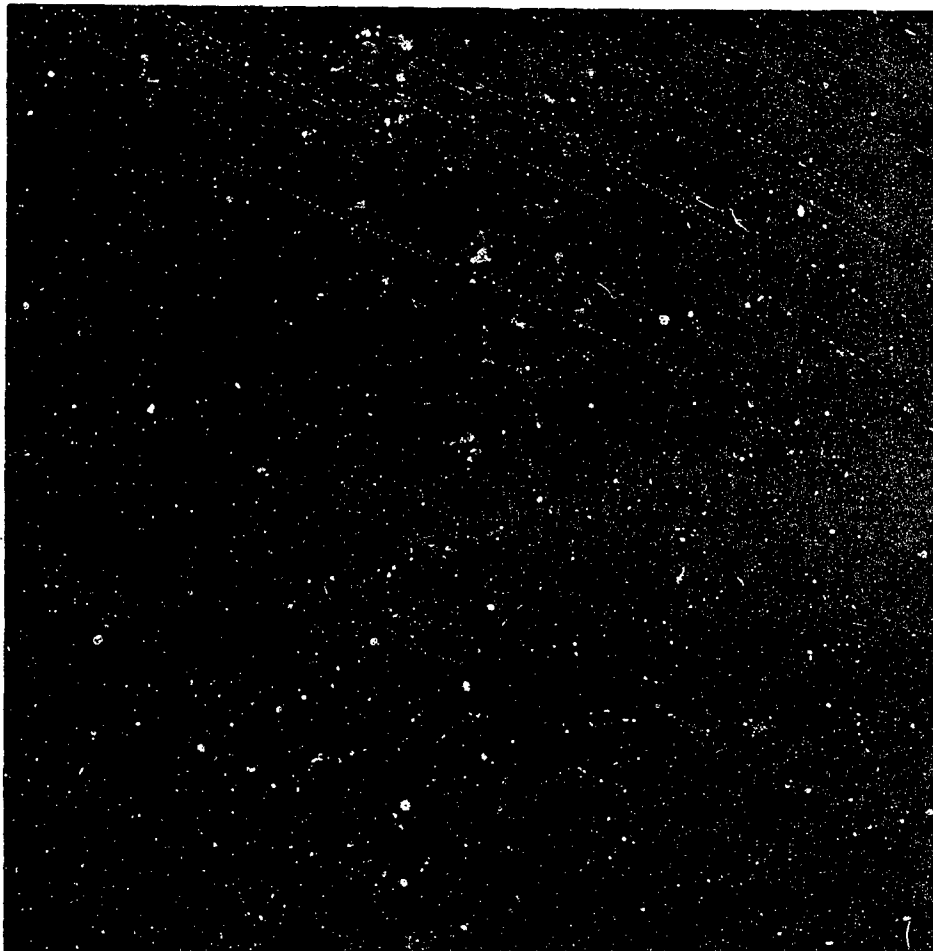


Heat E ---- 3" Thick Forging

100X

Figure 21. Composite Photograph Illustrating Shape and Orientation of Ferrite Plates

Top



Side

Front

Heat E ---- $1\frac{1}{2}$ " Thick Forging

100X

Figure 22. Composite Photograph Illustrating Shape and Orientation of Ferrite Plates

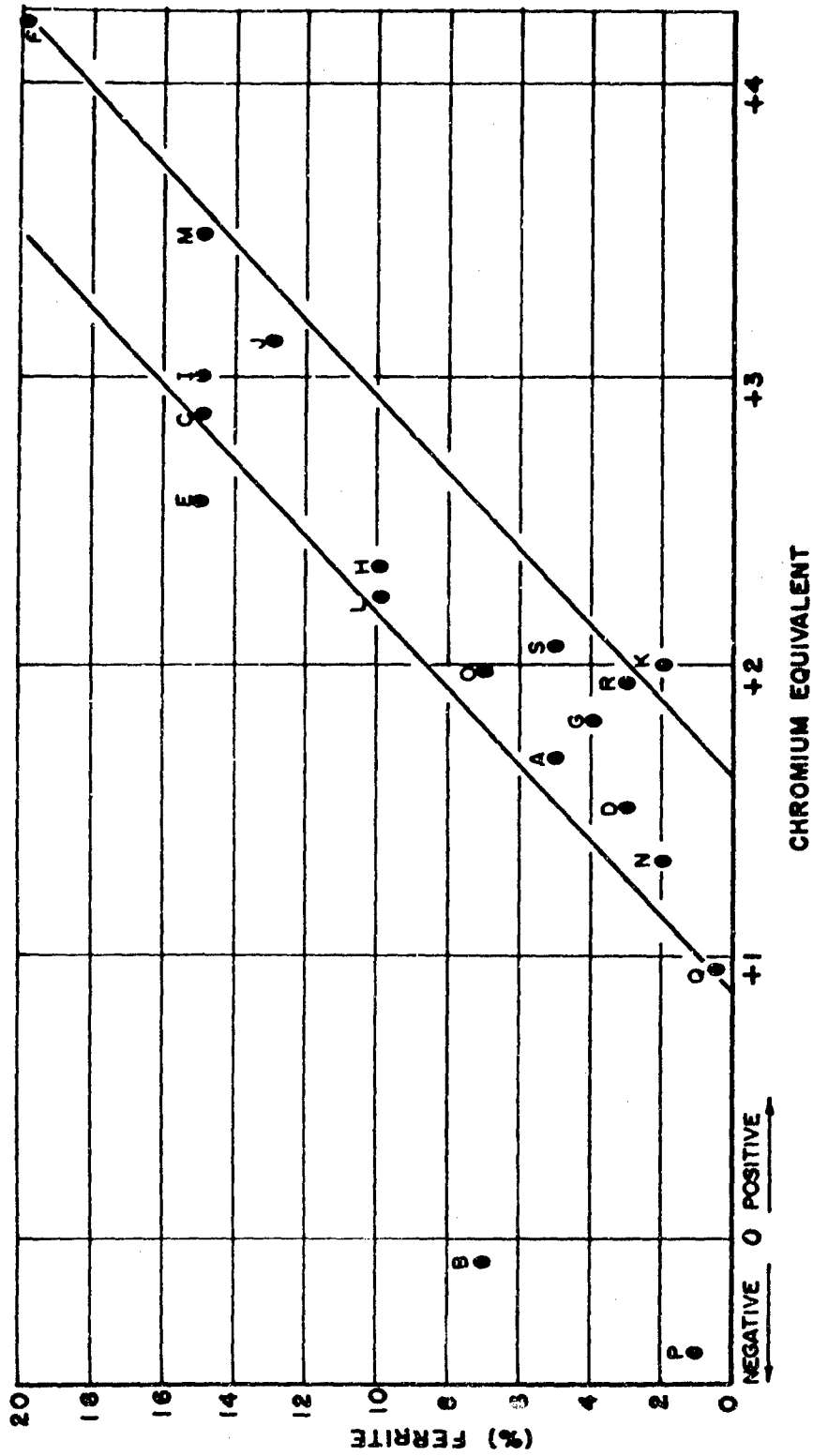


Figure 23. Percentage Ferrite as a Function of Chromium Equivalent

when compared to the normal transverse direction. This is particularly true of Heat B where there was no discernible ductility. (Micro-examination of the fracture in this instance revealed the presence of retained austenite. Krauss and Averbach¹ have shown that the presence of this phase is detrimental in steels of this type.) The reason for this anisotropy will be treated more fully in the next section.

B. Effect of Ferrite and Forging Reduction

It can readily be seen from examination of the data in Table III that there is no basic difference between edge, mid-radius and center locations. There is also no significant difference in strength (0.2% Y.S., U.T.S.) in the three directions (L, T, S) in the 5 inch thick forging of the lower ferrite heat. As the amount of reduction increases, however, a general increase in the strength level for all three directions with the transverse properties approximating those in the longitudinal direction and the short transverse strength showing only slightly lower values. This general increase can be attributed to effect of grain refinement as a result of the forging operation.

The data for the higher ferrite heat shows that although the initial strength level is comparable to that of the lower ferrite heat, it drops with increasing reduction. This is believed to be strictly associated with the higher volume of ferrite.

The effect of forging reduction upon ductility and impact strength is more prominent. Within a heat, at any reduction L T S for ductility (Elongation and Reduction of Area). The same relationship holds true for impact strength. As the amount of reduction increases, the T ductility parallels the L ductility while the S value falls off sharply. This anisotropy of properties can be definitely associated with the flattening of the ferrite plates.

Let us first examine the effect of directionality upon impact strength. If we mentally superimpose a ferrite plate upon Figure 3, we see that in order for fracture to occur in an L specimen, the ferrite plate itself must be sheared. In the S direction, since the plate is oriented in a direction parallel to the shear stress, the fracture can follow the ferrite grain boundary thus requiring less energy. In the case of the T specimen, the energy requirements would depend upon the width of the ferrite plate. With a relatively narrow plate, the case would be similar to that of the S specimen but as the width of the plate increases it would tend to approach the conditions in the L specimen.

Considering now the effect of directionality on ductility, it becomes apparent from comparing Figures 6 and 7 that as the ferrite level is increased, the divergence occurs with less reduction. To explain the above results a brief review of a recent theory of fracture mechanics proposed by G. R. Irwin² is presented. Irwin makes the assumption that all materials especially after fabrication into structures will have flaws

considerably larger than atomic dimensions. In failure of the structure at least one and probably many of the flaws, will start to grow slowly as the load is increased, until one such flaw reaches a critical size, at which time the rate of crack propagation increases by a large factor and failure results.

Much of this is predicated on earlier work by Griffith³ on fracturing in which he established the following relations.

$$\frac{de}{dA} = \frac{d}{dx} \left(\frac{\pi F^2 x^2}{E} \right) \quad \text{Where } de - \text{Release of strain energy}$$

$$\frac{dw}{dA} = \frac{d}{dx} \left(\frac{4Tx}{dx} \right) \quad dw - \text{Work done}$$

$$\quad \quad \quad dA - \text{Increment of fracture area}$$

$$E - \text{Young's modulus}$$

Griffith considered the work done dW as being expended against the surface tension and the total work done in enlarging the crack to length $2x$ as $4Tx$. When $\frac{de}{dA}$ becomes slightly larger than $\frac{dw}{dA}$, the crack propagates rapidly, driven by the release of strain energy.

The quantitative aspects of the stresses developed at the leading edges of the crack will not be touched upon here because it is believed that such a consideration is beyond the scope of this work and is not essential for the development of a gross explanation for the anisotropy encountered. What is necessary is the concept of a critical crack size and a mechanism initiating fracture.

Examination of the fractures as shown in Figures 24 through 27 revealed that there was no internal cracking of the ferrite but that cracking was occurring at the ferrite-martensite interface in a plane perpendicular to the applied stress. This fact is supported by the work of Dieter⁴ on 431 grade, the microstructure of which is not at all dissimilar in the hardened condition.

Essentially what is believed to happen is as follows:

Microcracks originate at the ferrite-martensite interface. With the application of increasing stress, these microcracks continue to expand along this interface until they are arrested by the martensite matrix at the end of the ferrite plate. When the width of the ferrite plate is less than some critical crack length characteristic of the interface then this growth is relatively slow, if however the ferrite width exceeds this critical crack size, the growth proceeds quite rapidly along the interface finally focusing very high stresses on the martensite at the terminal ends of the crack. The great concentration of ferrite surface in any plane perpendicular to the S direction allows the existence of only small volumes of martensite between the ferrite plates. This

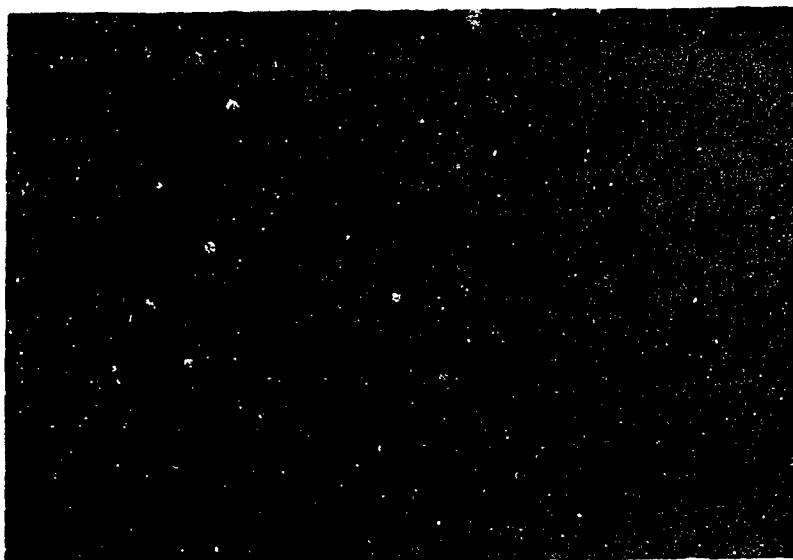


Figure 24 Short Transverse tensile
Heat E - 5" Thick Forging
Longitudinal Section through fracture
500X



Figure 25 Short Transverse tensile
Heat E - 3" Thick Forging
Longitudinal Section through fracture
500X

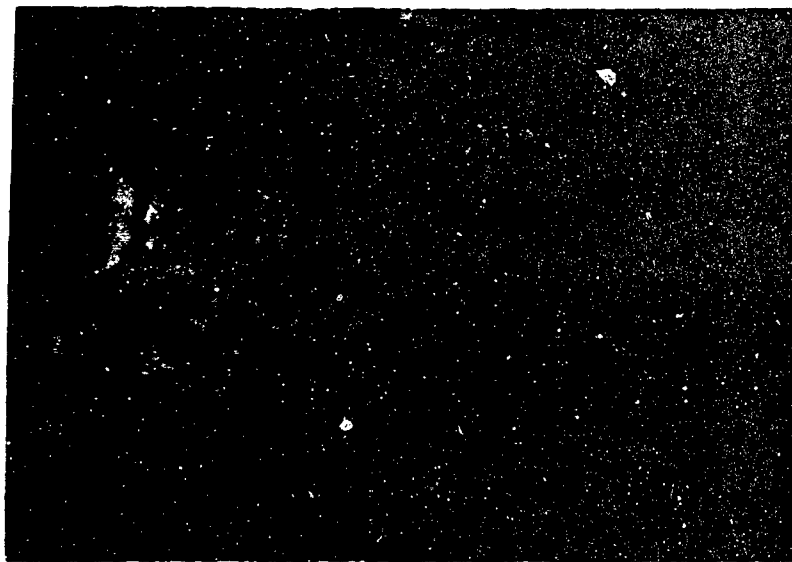


Figure 26 Short Transverse tensile
Heat D - 3" Thick Forging
Longitudinal Section through fracture
500X

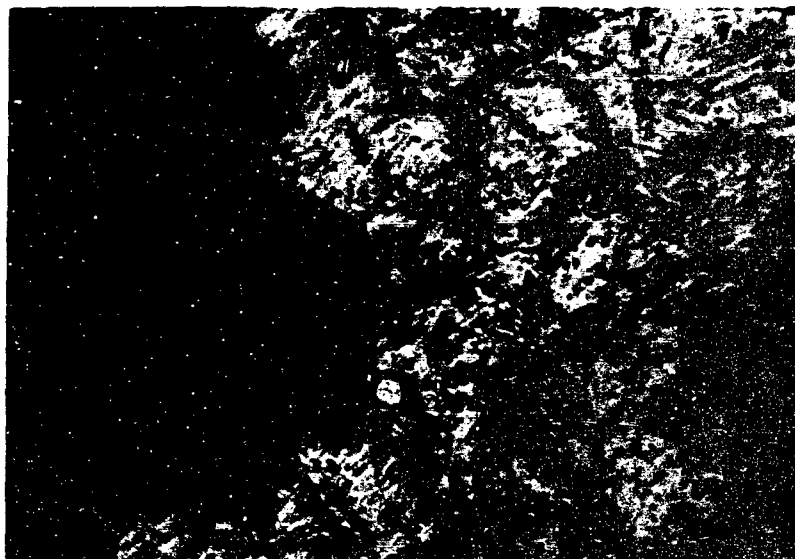


Figure 27 Short Transverse tensile
Heat D - 1½" Thick Forging
Longitudinal Section through fracture
500X

martensite can offer only limited resistance to the propagation of the rapidly converging cracks.

This orientation factor undoubtedly accounts for the poor ductility and toughness in the S direction since the maximum exposure of ferrite surface occurs in the plane normal to this direction. Much less ferrite is exposed in the T direction in any single plane and still less in the L direction.

With increasing amounts of ferrite less reduction is required to achieve a planar distribution of ferrite in the S direction and consequently a decrease in properties occurs such sooner.

C. Effect of Notch Orientation Upon Impact Strength

The data in Table IX clearly indicates that notch orientation affects the results obtained. The test values obtained with the notch perpendicular to the long transverse plane are constantly lower than those with the notch axis parallel. The notch parallel condition is the same as that discussed in subsection B, that is, that for failure to occur the ferrite plates must be sheared a relatively high energy requirement. In the notch perpendicular failure occurs by the tearing loose of ferrite from the matrix as shown in Figure 28. This latter condition apparently requires less energy than the former as evidenced by the results obtained.

D. Relationship of Heat Composition to Ferrite Content.

The plot of ferrite content versus chromium equivalent, indicates that there is basically a linear relationship. A rather wide band is evidenced, however, rather than a sharp line. There are a number of variables which might explain this result and should be considered with the thought of eliminating these possible errors on any further work. Perhaps the most prominent consideration is that the analytical samples were taken at random from the material and not from the exact location as the sample for the ferrite check. The possibility that some micro-segregation exists should not be excluded and in future work it would be wise to take both samples from the same location. The second and final consideration is the chemical analysis itself. In any analysis there is a limit to the reproducibility and in a study of this type any variation in analysis would tend to produce some scatter in the obtainable results.

The width of the band, however, precludes the exact prediction of ferrite content from heat analysis. What is indicated is that by stringent control of the heat chemistry the ferrite content can be minimized. This is particularly true of the nitrogen content. Nitrogen being a strong austenitizer exerts a marked effect on the ferrite content. Comparison of the chemistries of Heat D and Heat F shows that although the analysis are quite similar, except for nitrogen content, Heat F with a lower nitrogen content contains much more ferrite than does Heat D.

Longitudinal



Notch Perpendicular

Notch Parallel

Transverse



Notch Parallel

Notch Perpendicular

Figure 28. Fracture Surface of Longitudinal and Transverse Charpy V-Notch Specimens

The data shows one more point of interest; two heats, D and F, have negative chromium equivalents. These two heats fall well outside the plotted band. Both of these heats contained retained austenite. Thus, the necessity for maintaining a precise balance of elements is illustrated.

REFERENCES

1. Krauss, G., Jr., and Averbach, B. L., "Retained Austenite in Precipitation Hardening Stainless Steels." Transactions, American Society for Metals, Vol. 52.
2. Irwin, G. R., "Fracture Dynamics in Fracturing of Metals," Cleveland, American Society for Metals, 1948.
3. Griffith, A. A., "Phenomena of Rupture and Flow in the Solids," Physical Transactions, Royal Society of London, Vol. 221, p. 163, 1920
4. Dieter, G. E., "Effect of Microstructure and Heat Treatment on the Mechanical Properties of AISI Type 431 Stainless Steel," Transactions, American Society for Metals, Vol. 50, p. 722, 1958.

TABLE I

Mechanical Properties of Billet Stock

Heat	Ferrite	Direction	.02%Y.S. (Psi)	.2%Y.S. (Psi)	U.T.S. (Psi)	El. (%)	R.A. (%)
A	5%	Longitudinal	131,000	174,200	208,400	15.5	49.1
		"	133,300	174,200	206,800	17.0	51.3
		Transverse	127,300	171,900	209,500	10.0	19.0
		"	130,100	171,900	209,700	10.0	20.4
B	7%	Longitudinal	126,500	169,400	203,000	12.0	25.3
		"	133,100	171,700	204,000	13.0	26.7
		Transverse	131,500	172,100	205,200	3.0	6.2
		"	128,900	170,500	203,000	2.0	5.6
C	15%	Longitudinal	113,100	153,100	184,200	13.5	39.6
		"	117,600	155,300	186,400	13.0	43.7
		Transverse	109,100	147,500	182,600	3.0	2.4
		"	109,800	146,500	178,600	2.0	3.2

TABLE II

Mechanical Properties of 1½" Thick Flat Forgings

Heat	Direction	.02%Y.S. (Psi)	.2%Y.S. (Psi)	U.T.S. (Psi)	El. (%)	R.A. (%)
A	Transverse	134,600	177,600	210,300	12.0	28.1
	"	140,300	179,200	213,300	13.0	37.2
	Short Transverse	—	—	210,300	4.0	12.4
	"	—	—	208,700	5.0	17.4
B	Transverse	133,300	180,800	217,800	13.5	44.9
	"	140,300	182,800	218,000	13.5	44.3
	Short Transverse	—	—	204,800	*	*
	"	—	—	210,400	*	*
C	Transverse	120,200	159,700	189,700	16.5	50.7
	"	119,200	160,600	190,900	15.0	48.7
	Short Transverse	—	—	187,000	7.0	15.7
	"	—	—	185,100	5.0	23.1

*Not measurable

TABLE III

Heat D

Mechanical Properties of 5" Forging in Longitudinal, Transverse and Short Transverse Directions

<u>Location</u>	<u>Direction</u>	<u>.02%Y.S.</u> (Psi)	<u>.2%Y.S.</u> (Psi)	<u>T.S.</u> (Psi)	<u>El.</u> (%)	<u>R.A.</u> (%)	<u>Impact Strength</u> (ft.-lbs.)
Edge	L	141,600	166,150	178,350	21.5	54.1	19
	T	142,200	168,900	174,700	18.0	41.7	16
	S	142,200	168,700	184,750	18.0	26.5	3
Mid-radius	L	134,950	163,850	178,700	20.0	53.8	18
	T	144,600	166,300	178,700	19.0	41.7	8
	S	137,350	163,850	181,500	15.0	30.5	3
Center	L	137,500	159,000	172,700	20.0	52.2	18
	T	139,800	161,450	174,300	16.0	34.9	4
	S	137,350	163,850	181,550	15.0	28.5	3

TABLE IV

Heat D

Mechanical Properties of 3" Thick Forging in Longitudinal, Transverse and Short Transverse Directions

<u>Location</u>	<u>Direction</u>	<u>.02%Y.S.</u> (Psi)	<u>.2%Y.S.</u> (Psi)	<u>T.S.</u> (Psi)	<u>El.</u> (%)	<u>R.A.</u> (%)	<u>Impact Strength</u> (Ft.-lbs.)
Edge	L	145,800	166,300	180,700	20.0	53.8	22
	T	149,400	167,500	181,900	19.0	47.7	22
	S	139,800	159,000	177,100	16.4	31.7	4
Mid-radius	L	147,300	168,100	182,100	19.5	50.1	24
	T	145,700	167,500	178,800	18.5	46.9	19
	S	139,900	161,200	176,700	14.0	26.8	10
Center	L	148,200	166,300	180,700	20.0	55.4	32
	T	144,600	167,500	181,950	17.0	45.3	16
	S	140,950	159,000	177,100	15.0	29.7	5

TABLE V

Heat D

Mechanical Properties of 1½" Thick Forging in the
Longitudinal, Transverse and Short Transverse Directions

<u>Location</u>	<u>Direction</u>	<u>.02%Y.S.</u> (Psi)	<u>.2%Y.S.</u> (Psi)	<u>U.T.S.</u> (Psi)	<u>El.</u> (%)	<u>R.A.</u> (%)
Edge	L	151,100	180,600	195,000	19.0	55.0
	T	151,000	176,000	194,000	16.5	48.0
	S	150,000	176,000	192,000	6.0	23.5
Mid-radius	L	151,000	175,900	193,750	18.5	57.0
	T	150,000	177,000	194,000	19.0	47.0
	S	154,000	170,000	188,000	7.5	28.5
Center	L	151,000	175,000	191,500	20.0	53.0
	T	153,500	178,000	195,000	18.7	47.0
	S	153,500	170,000	186,000	5.0	20.0

TABLE VI

Heat E

Mechanical Properties of 5" Thick Forging in the
Longitudinal, Transverse and Short Transverse Directions

<u>Location</u>	<u>Direction</u>	<u>.02%Y.S.</u> (Psi)	<u>.2%Y.S.</u> (Psi)	<u>U.T.S.</u> (Psi)	<u>El.</u> (%)	<u>R.A.</u> (%)	<u>Impact Strength</u> (ft.-lb.)
Edge	L	145,700	171,100	185,150	20.0	54.4	20
	T	149,400	172,300	185,150	15.0	39.9	15
	S	142,150	168,700	183,550	10.0	16.6	4
Mid-radius	L	146,900	172,500	184,700	21.5	55.6	23
	T	151,300	174,500	183,500	16.0	36.8	14
	S	149,500	173,600	185,300	11.5	15.7	5
Center	L	147,200	172,100	181,700	20.0	53.8	25
	T	153,000	174,700	185,950	15.0	33.7	16
	S	143,400	171,000	184,350	13.0	11.4	4

TABLE VII

Heat E

Mechanical Properties of 3" Thick Forging in the
Longitudinal, Transverse and Short Transverse Directions

<u>Location</u>	<u>Direction</u>	<u>.02%Y.S.</u> (Psi)	<u>.2%Y.S.</u> (Psi)	<u>U.T.S.</u> (Psi)	<u>El.</u> (%)	<u>R.A.</u> (%)	<u>Impact Strength</u> (ft.-lb.)
Edge	L	147,900	166,300	174,700	18.0	56.6	19
	T	151,800	171,100	179,900	16.0	40.7	20
	S	151,000	165,000	179,900	7.4	12.4	4
Mid-radius	L	147,500	168,300	174,700	19.0	51.7	21
	T	148,800	163,850	175,900	18.0	41.1	18
	S	149,500	165,000	179,900	8.0	15.5	3
Center	L	147,900	171,300	175,200	18.5	48.3	22
	T	149,400	168,700	180,300	15.0	37.5	19
	S	148,800	166,500	179,800	6.6	11.5	5

TABLE VIII

Heat E

Mechanical Properties of 1½" Thick Forging in the
Longitudinal, Transverse and Short Transverse Directions

<u>Location</u>	<u>Direction</u>	<u>.02%Y.S.</u> (Psi)	<u>.2%Y.S.</u> (Psi)	<u>U.T.S.</u> (Psi)	<u>El.</u> (%)	<u>R.A.</u> (%)
Edge	L	137,300	153,000	170,300	18.0	57.0
	T	128,900	147,000	169,900	16.0	45.3
	S	124,500	136,000	164,000	7.5	12.2
Mid-radius	L	137,300	153,000	168,300	20.0	53.8
	T	137,300	150,600	170,300	17.0	45.3
	S	124,000	139,000	161,000	5.0	11.4
Center	L	138,500	152,100	171,200	19.0	54.3
	T	137,300	151,400	168,700	16.5	44.0
	S	127,300	146,400	104,300	6.0	8.1

TABLE IX

Effect of Notch Orientation upon Impact Tests
 Material: 3"x1" flat bar — Charpy V-Notch specimens

Longitudinal Tests

<u>Heat No.</u>	<u>Orientation</u>	<u>Impact Strength (ft.-lbs.)</u>
C	Parallel	25
C	"	25
F	"	13
F	"	12
		<u>18.7</u> Average
C	Perpendicular	13
C	"	15
F	"	8
F	"	10
		<u>11.5</u> Average

Transverse Tests

<u>Heat No.</u>	<u>Orientation</u>	<u>Impact Strength (ft.-lbs.)</u>
C	Parallel	6
C	"	6
C	"	6
F	"	7
F		<u>6.25</u> Average
C	Perpendicular	5
C	"	5
C	"	6
F	"	4
F		<u>5.0</u> Average

TABLE X

Chemical Analysis, Ferrite Content
and Chromium Equivalent
for
Eighteen Random Heats

Heat	Analysis							Ferrite (%)	Cr Equiv.
	C	Mn	Si	Cr	Ni	Mo	N		
A	.125	1.02	.34	15.74	4.32	2.70	.086	5	/1.68
B	.128	.97	.32	15.50	4.20	3.00	.091	7	-0.15
C	.136	.79	.38	15.52	4.37	2.94	.043	15	/2.86
D	.128	.99	.37	15.72	4.29	2.70	.099	3	/1.51
E	.149	.92	.35	15.64	4.14	2.90	.084	15	/2.56
F	.122	.73	.31	15.52	4.27	2.94	.051	20	/4.19
G	.111	.70	.33	14.97	4.31	2.66	.087	4	/1.80
H	.121	.97	.31	15.74	4.14	2.70	.091	10	/2.33
I	.123	.92	.38	15.20	4.18	2.88	.084	15	/3.00
J	.103	1.00	.34	15.72	4.10	2.94	.087	13	/3.13
K	.141	.86	.40	15.00	4.31	2.90	.080	2	/2.00
L	.116	.57	.21	15.50	4.35	2.70	.072	10	/2.22
M	.116	.99	.37	15.64	4.20	2.84	.077	15	/3.49
N	.125	1.01	.40	15.38	4.32	2.58	.082	2	/1.34
O	.150	.95	.42	15.73	4.18	2.82	.098	7	/1.97
P	.117	1.06	.35	15.42	4.75	2.58	.081	1	-0.15
Q	.116	.95	.35	15.56	4.45	2.60	.043	1	/0.93
R	.122	.92	.31	15.46	4.25	2.70	.082	3	/1.94
S	.113	1.01	.34	15.30	4.29	2.70	.079	5	/2.07

APPENDIX

METHOD OF DETERMINATION OF PERCENTAGE OF FERRITE IN MICROSTRUCTURES BY GRID METHOD

This is a method for determining the percentage of ferrite in an austenitic or tempered martensitic structure by microscopic examination developed by F. D. Moore of Allegheny Ludlum Steel Corporation, Watervliet New York. It has been used to obtain reproducible results and the correlation of these results between various personnel performing the ratings has been quite acceptable.

Procedure

Take micro-specimens longitudinally to direction of rolling. Prepare metallographically and etch with any etchant which will clearly delineate the ferrite stringers. Use a transparent grid, ruled off in $1/4$ inch squares, on the ground glass of the metallograph to view the ferrite fields. A magnification of 100X or 200X is most commonly used and approximately 10 random fields are rated using their average as the ferrite content of the micro-sample.

An estimation of the width of the ferrite stringers is probably the most critical part of the method as it is dependent on human interpretation or opinion. It is arrived at by scanning the field to be examined and comparing the widths with the $1/4$ inch squares. It is then relatively easy to determine if they cover a $1/4$, $1/3$, or $1/2$ square and use the appropriate width fraction in the final determination. Estimation of the width becomes quite easy and accurate after working with the grid for awhile.

The actual determination of the percentage of ferrite in a particular field is not taken as follows:

A count is made of each $1/4$ inch segment of the vertical line which intersects a ferrite stringer or island, thereby arriving at a total number of intersections.

Multiply the number of intersections by $1/4$ inch (the spacing between the vertical lines) to obtain the approximate length of the ferrite in the field; by the estimated width of the ferrite; thereby arriving at the approximate total area of the ferrite present in the field in square inches

Divide the total area of the ferrite by the total area of the field, thereby arriving at the percentage of ferrite present in the field.

Attached are photomicrographic (Figure 29) illustrating the use of this method and the percent of ferrite determined to be present in the field. At the side of each photograph is the number of intersections

APPENDIX (Continued)

counted in each 1/4 inch wide horizontal segment with the total number of intersections at the bottom.

As an example of the actual use of the method, using the first illustration, the ferrite percentage of that field would be determined as follows:

Multiply the total number of intersections (111) by the spacing between the vertical lines (1/4") by the estimated width of the ferrite (1/16");

$$111 \times 1/4" \times 1/16" = 111/64 = 1.73 \text{ square inches.}$$

Divide the total area of the ferrite (1.73 sq. in.) by the total area of the field (3.5" x 3.5" = 12.25 sq. in.);

$$\frac{1.73 \text{ sq. in.}}{12.25 \text{ sq. in.}} = 14.2\% \text{ ferrite present in this field}$$

It is an obvious conclusion that the accuracy of this method and the correlation of results would be dependent on several factors, such as adjacent sampling, preparation of specimens and proficiency in estimation of width of ferrite.

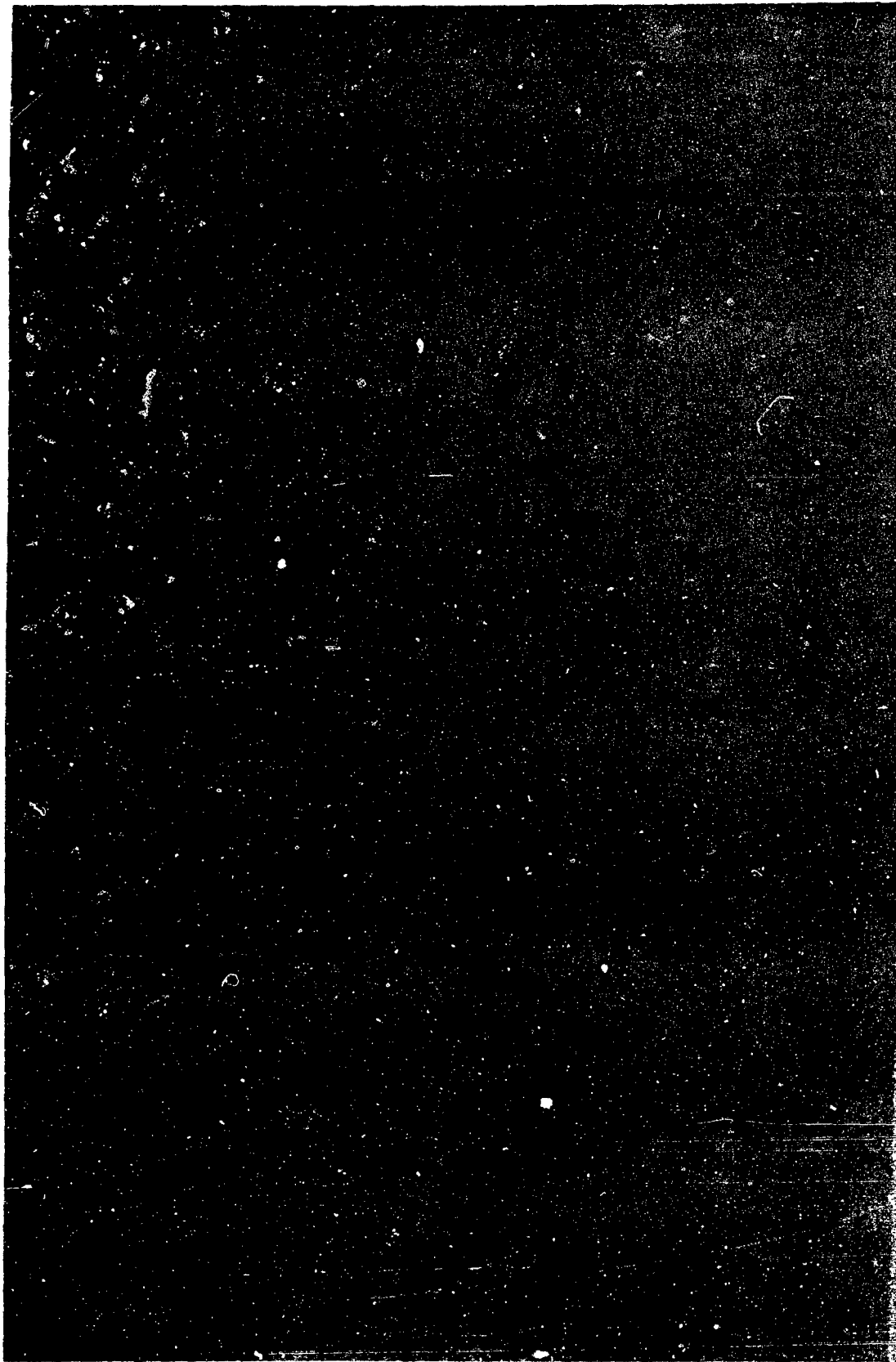


Figure 29. Photomicrographs Illustrating the Grid Method

DISTRIBUTION LIST

Copies

Commanding General

ATTN: AMSWE-LCD

OR

RD

RDA

RDQ

RDR

U. S. Army Weapons Command

Rock Island Arsenal

Rock Island, Illinois, 61202

Commanding General

ATTN: AMCRD-DE

AMCRD-RS-CM

Room 2502, Bldg, T-7

U. S. Army Materiel Command

Washington, D. C., 20315

Commanding General

ATTN: Dr. C. Pickett AMXCC

Technical Library

Aberdeen Proving Ground, Maryland, 21005

Commanding General

ATTN: AMSMO

U. S. Army Mobility Command

Warren, Michigan, 48090

Commanding General

ATTN: Documentation & Technical Information Branch

Mr. E. E. Ely, AMSMI-RRS

Mr. R. Fink, AMSMI-RKY

Mr. W. I. Thomas, AMSMI

Mr. E. J. Sheelahan, AMSMI-RSM

U. S. Army Missile Command

Redstone Arsenal, Alabama, 35809

Commanding Officer

Harry Diamond Laboratories

ATTN: Library

Washington, D. C., 20438

Commanding Officer

U. S. Army Research Office (Durham)

Box CM, Duke Station

Durham, North Carolina, 27706

Commanding Officer ATTN: AMXR-Technical Information Center U. S. Army Materials Research Agency Watertown, Mass., 02172	2
Commanding Officer ATTN: SMUFA Frankford Arsenal Philadelphia, Pa., 19137	1
Commanding Officer ATTN: SMUPA Picatinny Arsenal Dover, New Jersey, 07801	1
Commanding Officer ATTN: SWERI-RDD Rock Island Arsenal Rock Island, Illinois, 61202	1
Commanding Officer ATTN: SWESP-PRD Springfield Armory Springfield, Mass., 01101	1
Commanding Officer ATTN: SMIWT-EX Watertown Arsenal Watertown, Mass., 02172	1
Commanding Officer ATTN: Materials Branch U. S. Army Signal R&D Laboratory Fort Monmouth, N. J., 07703	1
Commander ATTN: Mr. M. E. Jansson-1065 Technical Library Office of Naval Research Department of the Navy Washington 25, D. C.	1
Commander ATTN: Technical Information Center Wright Air Development Division Wright-Patterson Air Force Base, Ohio	3
Commander ATTN: Technical Information Section Defense Documentation Center Cameron Station Alexandria, Virginia, 22314	20

Office of Technical Services Department of Commerce Washington 25, D. C. ATTN: Chief, Acquisition Section - Annex-1	2
Robert L. Shannon, Extension Manager U. S. Atomic Energy Commission Division of Technical Information Extension P. O. Box 62 Oak Ridge, Tennessee, 37831	2
Commandant ATTN: Office of the Librarian Hq. U. S. Army Aviation School Fort Rucker, Alabama	2
U. S. Army Engineer Research and Development Laboratories ATTN: STINFO Branch Fort Belvoir, Virginia	2
Office of Technical Services Department of Commerce 1200 S. Eads St., Arlington, Va. ATTN: OTS Stock	50